

1 Resource asynchrony and landscape homogenization as drivers of virulence

2 evolution

3 Tobias Kürschner<sup>1,2</sup>, Cédric Scherer<sup>2</sup>, Viktoriia Radchuk<sup>2</sup>, Niels Blaum<sup>1</sup>, Stephanie Kramer-

4 Schadt<sup>2,3</sup>

5 <sup>1</sup> University of Potsdam, Plant Ecology and Nature Conservation, Potsdam, Germany

6 <sup>2</sup> Leibniz Institute for Zoo and Wildlife Research, Department of Ecological Dynamics, Berlin, Germany

7 <sup>3</sup> Technische Universität Berlin, Institute of Ecology, Berlin, Germany

8 Keywords: virulence, evolution, host-pathogen dynamics, dynamic landscapes, global change

9

## 10 Abstract

11 In the last years, the emergence of zoonotic diseases and the frequency of disease outbreaks  
12 have increased substantially, fuelled by habitat encroachment and asynchrony of biological  
13 cycles due to global change. The virulence of these diseases is a key aspect for their success.  
14 In order to understand the complex processes of pathogen virulence evolution in the global  
15 change context, we adapted an established individual-based model of host-pathogen  
16 dynamics. Our model simulates a population of social hosts affected by an evolving pathogen  
17 in a dynamic landscape. Pathogen virulence evolution is explored by the inclusion of multiple  
18 strains in the model that differ in their transmission capability and lethality. Simultaneously,  
19 the host's resource landscape is subjected to spatial and temporal dynamics, emulating effects  
20 of global change.

21 We found an increase in pathogenic virulence and a shift in strain dominance with increasing  
22 landscape homogenisation. Our model further shows a trend to lower virulence pathogens  
23 being dominant in fragmented landscapes, although pulses of highly virulent strains are  
24 expected under resource asynchrony. While all landscape scenarios favour coexistence of low  
25 and high virulent strains, when host density increases, the high virulence strains capitalize on  
26 the high possibility for transmission and are likely to become dominant.

27

## 28 Author Summary

29 Disease outbreaks primarily caused by contact with animals are increasing in recent years,  
30 related to habitat destruction and altered biological cycles due to climate change. Pathogens  
31 associated with such outbreaks will be more successful the more effectively they can spread  
32 in a population. Thus, understanding the conditions over which those pathogens evolve will  
33 help us to limit the impact of disease outbreaks in the future. To this end, we used an  
34 individual based model that allowed us to study different scenarios. Our model had three  
35 main components: a host-pathogen system, a dynamic resource landscape with different  
36 degrees of fragmentation and temporal resource mismatches. We used dynamic landscapes  
37 with varying resource amounts over the years and consisting of multiple large or smaller  
38 habitat clusters. Our simulations showed that homogenous landscapes resulted in higher  
39 virulent pathogens and fragmented landscapes in lesser virulent pathogens. However, across  
40 all scenarios, high and low virulent pathogen strains were able to coexist.

## 41 Introduction

42

43 A key aspect of the invasive success of infectious pathogens such as Ebola, SARS-CoV-2 or  
44 Avian Influenza in a host population is the mastering of the delicate interplay of transmission  
45 and host exploitation, also termed virulence. To persist, a pathogen must find the balance  
46 between quick replication and growth in the host often resulting in severe infections killing  
47 its host while still being able to spread across timescales (Visher et al. 2021). This intricate  
48 balance can only be kept up by an arms race between hosts' immune reactions and strategies  
49 of the pathogen to evade and counteract host resistance, termed adaptive evolution of  
50 virulence (Cressler et al. 2016). This leads to the emergence of ever-new pathogenic strains  
51 from the wild strain with modulated pathogenic traits, and if the new strain manages to  
52 establish, this might have unforeseeable effects on host population and disease dynamics.

53

54 Both transmission and virulence are integrally tied to density and spatiotemporal distribution  
55 of host individuals (Alizon et al. 2009, Cressler et al. 2016), which in return are subject to  
56 habitat configuration and spatiotemporal variation in resource availability.

57 Global change might exacerbate disease dynamics in the near future, facilitated by land-use  
58 change, habitat encroachment, or climate warming (Patz et al. 2004, Wilcox and Gubler  
59 2005). These disturbances will severely influence disease outbreaks by changes in the life  
60 history, density and availability of hosts as well as feedbacks on the landscape level due to  
61 asynchrony in timescales (Kürschner et al. 2021). In this context, it is particularly important  
62 to not only understand factors that govern the spread and the persistence of pathogens in  
63 changing landscapes to put counteractive measures in place (Griette et al. 2015), but to also

64 understand how these factors reciprocally influence the adaptive potential of pathogenic  
65 traits.

66

67 Virulence evolution is often highly accelerated during the emergence or invasion stage of an  
68 epidemic (Griette et al. 2015, Geoghegan and Holmes 2018). The emergence stage is  
69 characterized by a high number of susceptible —and later infected— host individuals  
70 associated with a high number of mutations due to the steep increase of infected individuals  
71 (Galvani 2003). Since the distribution of host individuals in a landscape determines the  
72 number of available susceptible individuals, local and regional host densities are important  
73 factors in the evolution of virulence (Boots 2004). With global change further altering the  
74 resource distribution in space and time, subsequent changes in the spatiotemporal density and  
75 distribution of host individuals (Galvani 2003, Boots 2004, Geoghegan and Holmes 2018)  
76 could influence the evolution of virulence. Density changes could for example be induced via  
77 mismatches between the host's life history such as reproduction and host resource availability  
78 at that time.

79

80 Theory predicts an evolution towards low virulence through altered habitat configuration or  
81 host density distribution (Boots and Meador 2007, Cressler et al. 2016). Virulence has been  
82 shown to be adaptive if there is a correlation with other pathogenic traits such as  
83 contagiousness, which is known as virulence-transmission trade-off hypothesis (Day 2003).  
84 The transmission-virulence trade-off hypothesis states that an increase in strain transmission  
85 causes shorter infections through higher lethality (Anderson and May 1982, Alizon and  
86 Michalakis 2015). In other words, pathogen virulence is subject to a variety of evolutionary  
87 trade-offs (Kamo et al. 2007, Messinger and Ostling 2009, Cressler et al. 2016).

88

89 The theoretical models of virulence evolution, particularly the classical adaptive dynamics  
90 framework, rely on the assumption that mutation of pathogens happens very slowly and that  
91 mutations towards new strains can only occur after the dominant strain has reached  
92 equilibrium (Dieckmann et al. 2005). However, such simplified assumptions are rarely  
93 applicable to pathogens in nature, which often undergo transient dynamics, for example due  
94 to temporal and spatial changes in the landscape structure. Due to temporal variation in the  
95 landscape, the formation of spatial (figure 1 a) and or temporal (figure 1 b) host niches can  
96 cascade through the density distribution of potential hosts onto host-pathogen interactions  
97 (figure 1 c, d). The formation of niches with varying beneficial or detrimental properties for  
98 host and pathogen could facilitate the appearance of different pathogenic strains at specific  
99 times or locations. The result can be a complex system of different competing and coexisting  
100 pathogen strains (figure 1 e) with their own spatial and temporal dynamics. The constant  
101 emergence, re-emergence, and extinction of pathogenic strains will result in an overlap and  
102 possible coexistence between different strains, all competing for the same resource (Choua  
103 and Bonachela 2019).

104 While theoretical studies focus on long-term predictions of pathogenic strains with  
105 evolutionarily stable virulence at equilibrium (Lenski and May 1994, Day and Gandon 2007),  
106 there is a lack of knowledge linking complex dynamics arising from global change to the  
107 evolution of virulence through space and time during an epidemic (Lebarbenchon et al.  
108 2008). Also, links between resources and host density are rarely incorporated into  
109 evolutionary models, which typically assume that host density remains at equilibrium [3,28 in  
110 Hite&Cressler2018]. A prominent example tackling the evolution of virulence in changing  
111 host densities due to changes in resources is the work of Hite & Cressler (2018). They  
112 revealed complex effects of host population dynamics on parasite evolution, including

113 regions of evolutionary bistability, where parasites ‘rode the cycles’ of their hosts and phases  
114 with high host exploitation superseded phases of low virulence (Hite & Cressler 2018).

115

116 Here, we go one step beyond the important link between host ecology and parasite evolution  
117 by asking what effect heterogeneously distributed and dynamic resources will pose on the  
118 evolution of virulence, particularly how temporal mismatches between optimal resource  
119 availability and biological events, such as reproduction, affect host-pathogen coexistence and  
120 pathogen spread through adaptive virulence dynamics. To this end, we modified an existing  
121 spatially-explicit individual-based host-pathogen model of a group-living social herbivore  
122 (Kramer-Schadt et al. 2009, Lange et al. 2012a, b, Scherer et al. 2020, Kürschner et al. 2021)  
123 and added evolution in pathogen traits leading to multi-strain outbreak scenarios. In  
124 accordance with theory, we have already shown for a static host exploitation rate that  
125 pathogen extinction is higher in landscapes with randomly distributed and fluctuating  
126 resources, but that the formation of disease hotspots form an epidemic rescue for the  
127 pathogen when hosts are mobile (Kürschner et al. 2021).

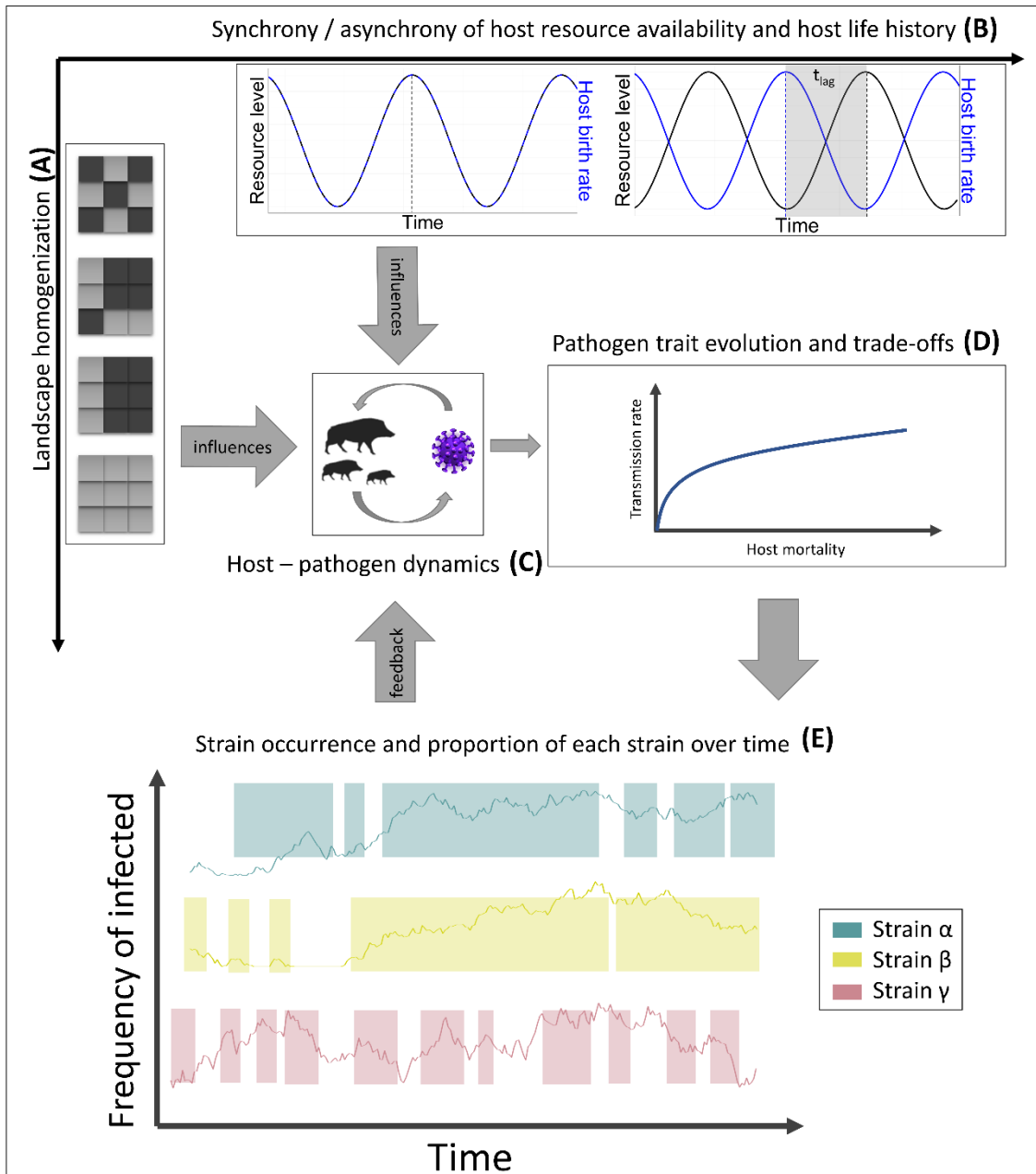
128

129 We here hypothesized that dynamic landscapes induce evolution in pathogenic virulence to  
130 facilitate host-pathogen coexistence (H1). In more detail, we expect pathogenic virulence to  
131 evolve into a system of different viral strains that will coexist and persist within the host  
132 population in parallel (prediction 1). We also predict that the frequency of ‘host cycle riding’  
133 pathogenic strain emergence will be larger under environmental uncertainty, hence global  
134 change effects might lead to higher pathogenic strain emergence (prediction 2), i.e. with a  
135 higher chance for spill-over events.

136

137 We further hypothesize that due to the destabilisation of the host population under  
138 asynchronous dynamics, virulence will evolve to lower levels than under homogeneous and  
139 stable resource availability (H2). We expect increasing landscape homogenization and related  
140 contact homogenization to facilitate evolution towards higher pathogenic virulence by  
141 increasing the availability of hosts for highly virulent strains (prediction 3), with few  
142 dominant strains governing the dynamics for a long time (prediction 4).  
143





144

145 *Figure 1: Conceptual figure: Landscape homogenization (A) and synchrony/asynchrony ( $t_{lag}$ )*  
146 *of host life-history and host-resource availability (B) influence host-pathogen dynamics (C)*  
147 *and subsequently the evolution of pathogenic traits (D) that will affect strain occurrence over*  
148 *time where gaps in the background line are times when the strain did not occur in the*  
149 *landscape (E).*

150

## 151 Results

### 152 **Host-pathogen coexistence**

153 Overall, host pathogen coexistence  $P_{\text{coex}}$  was very high in almost all tested scenarios. Due to a  
154 collapse of the host population in asynchronous scenarios in homogeneous landscapes, host-  
155 pathogen coexistence was not achievable in the current model-framework and this single  
156 scenario therefore excluded. We did not find notable differences in the other scenarios  
157 (Appendix Fig. B2).

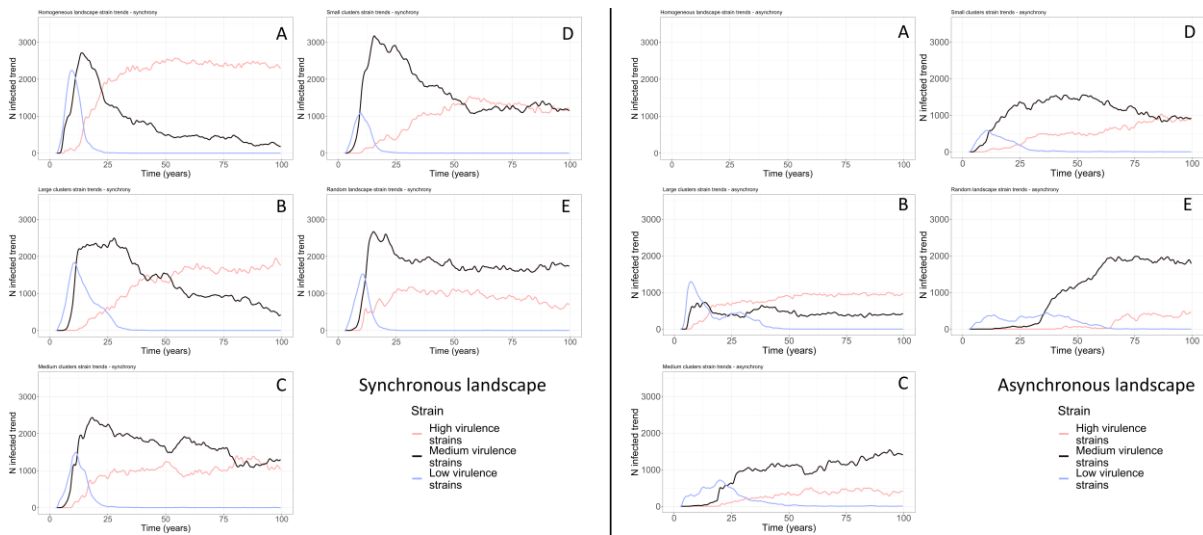
### 158 **Categorized infection trends**

159 Our model showed that in synchronous scenarios, highly virulent strains were the least  
160 abundant ones among the three strain categories during the early stages of the epidemic.  
161 However, these strains became dominant in the later stages of the epidemic in homogeneous  
162 and large clustered landscapes (figure 2, left). With increasing landscape homogenization,  
163 medium virulence strains in the later stages of the epidemic were usually dominating along  
164 with high virulence strains. Across all landscapes, low virulent strains only occurred in high  
165 prevalence in the early stages of the epidemic but reached higher prevalence in less  
166 heterogeneous landscapes.

167

168 In scenarios with asynchrony, low virulent strains occurred over a longer time period and  
169 were more prevalent in the host population, while medium and highly virulent strains  
170 occurred later at high prevalence (figure 2, right). Furthermore, prevalence of all strain  
171 categories was lower throughout the simulations when directly compared to the  
172 ‘synchronous’ scenarios. A clear shift towards a dominance of highly virulent strains only  
173 occurred in the less heterogeneous, large clustered landscapes.

174



175

176 *Figure 2: Temporal trends of the number of hosts infected with the strains of three virulence*  
 177 *categories, low (blue) medium (black) and high (red) virulence over time. The left half shows*  
 178 *the trends for synchronous host reproduction ( $t_{lag} = 0$ ) and the right half for asynchronous*  
 179 *host reproduction ( $t_{lag} = 100$ ) scenarios.*

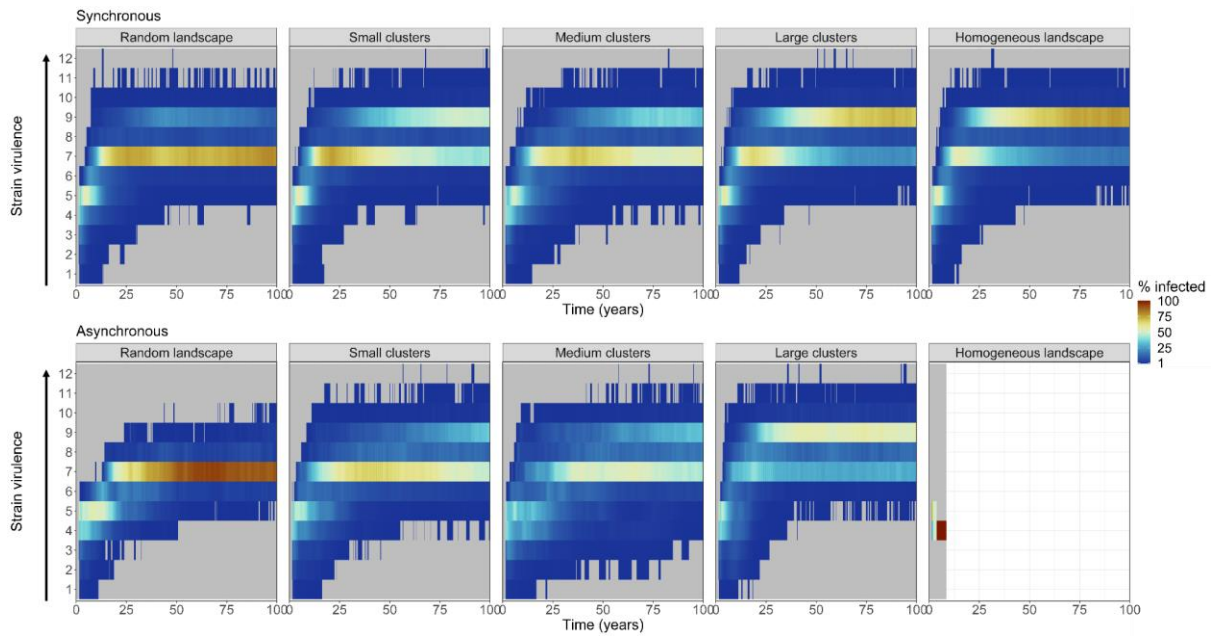
180 Strain specific occurrence and dominance over time

181 Strain occurrence and dominance of high virulent strains decreased with increasing landscape  
 182 heterogenization in dynamic landscapes in combination with synchronous scenarios (figure 3  
 183 top). In the highly heterogeneous random landscape, low virulent strains persisted longer  
 184 while higher virulent strains occurred much later in time (around year 40), compared to the  
 185 same landscape in synchronous scenarios. After its appearance through mutations around  
 186 year 45, the medium virulent strain 7 became dominant for the course of the epidemic. As  
 187 landscape homogeneity increased (from random landscapes to small clustered landscapes),  
 188 lower virulent strains occurred on much shorter time spans. The high virulent strains  
 189 appeared much earlier around year 10 of the epidemic and remained present in the landscape  
 190 for the duration of the simulation. A further increase in homogenization towards medium-  
 191 sized patches showed overall similar patterns as the small clustered landscape with the

192 exception of the strain 7 peak prevalence, which shifted towards the end of the epidemic. In  
193 the highly homogenous large clustered landscapes, the lower virulent strains persisted for a  
194 longer period, while medium virulent strains were represented during the full period of the  
195 epidemic. Contrary to the more heterogeneous landscapes, strain 7 did not become the  
196 dominant strain despite high prevalence in the host population. As indicated by the larger  
197 proportion of hosts infected with higher virulent strains, overall, in synchronous scenarios  
198 (figure 3), virulence of occurring strains increased over time and with increasing landscape  
199 homogenization. In asynchronous scenarios we observed a similar increase in strain  
200 occurrence with landscape homogenization, even though the temporal rate of increase was  
201 smaller compared to synchronous scenarios. Furthermore, there was a temporal variation of  
202 strain occurrence within the more homogenous landscape between synchronous and  
203 asynchronous scenarios, as can be seen in a direct comparison of the per-strain infection  
204 counts and wavelets of synchronous and asynchronous scenarios over time (figure 4). A  
205 general comparison of the proportional strain contribution in asynchronous vs synchronous  
206 scenarios further showed that the occurring strains were of lower virulence in asynchronous  
207 scenarios in case of the more heterogeneous landscapes (Appendix Fig.B3).

208

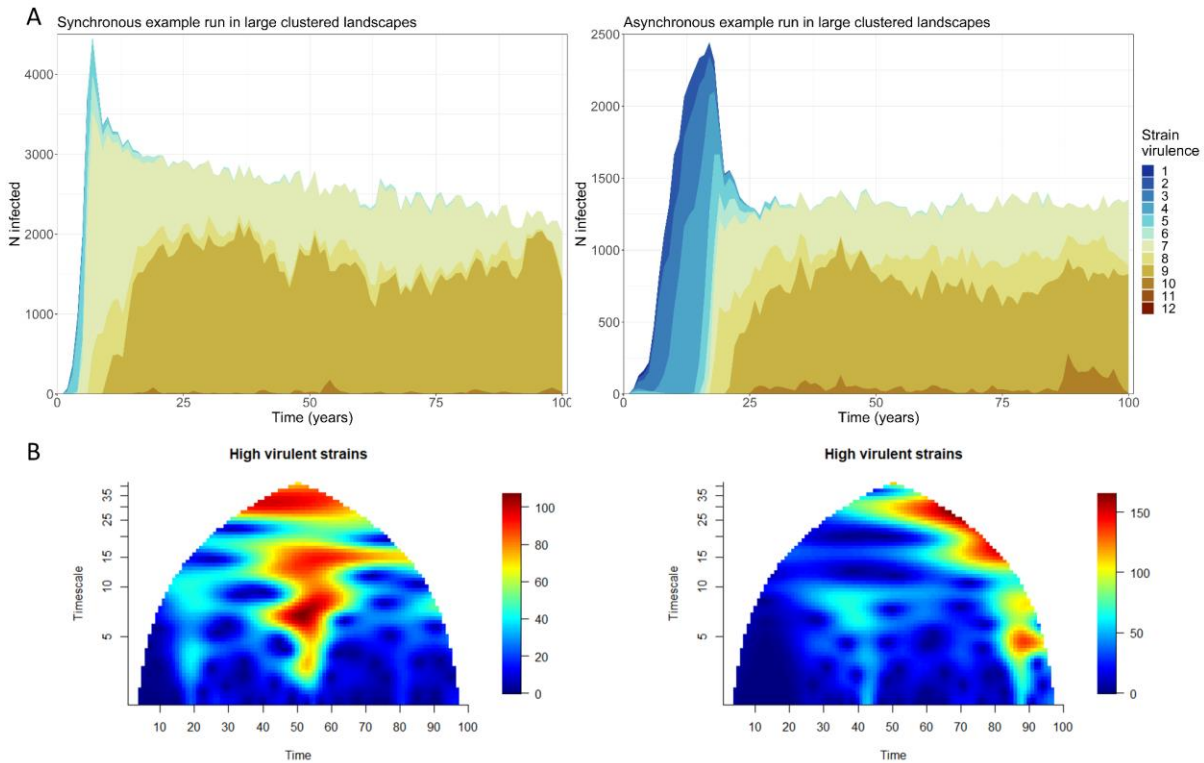
209



210

211 *Figure 3: Occurrence and dominance of the different virulence strains in synchronous ( $t_{lag} =$*   
212 *0, top row) and asynchronous ( $t_{lag} = 100$ , bottom row) scenarios. Colour gradient represents*  
213 *the proportion of infected individuals with each strain in the landscape. Grey areas represent*  
214 *zero occurrence of the strains.*

215



216

217 *Figure 4: A-Muller plot for a single example run in a large clustered landscape in*  
218 *synchronous (left) and asynchronous (right) scenarios, showing the number of infected*  
219 *individuals for each strain (colour) over time aggregated as annual mean. B- Wavelet*  
220 *analysis of high virulent strains in synchronous (left) and asynchronous (right) scenarios of a*  
221 *single example run in a large clustered landscape using the R package “wsyn” [49].*

222 Discussion

223 To extend the understanding of pathogen evolution and spread during epidemics, we  
224 implemented virulence evolution in an individual-based model simulating an interdependent,  
225 tri-trophic system (landscape resources - host - pathogen) under the effects of global change.  
226 In accordance with our hypotheses, we found an increase in pathogenic virulence and a shift  
227 in strain dominance with increasing landscape homogenisation.

228 Landscape homogenisation alters the density distribution of susceptible host individuals by  
229 increasing host connectivity, which subsequently can lead to more infection events and viral  
230 mutations. The detrimental effect that density, connectivity and contact rates can have on  
231 viral mutations and infection events can also be observed in “superspreader”-events of the  
232 current SARS-CoV-2 pandemic (Tasakis et al. 2021). Our results support that host density  
233 and connectivity are the most important factors that affect the emergence of high virulence in  
234 directly transmitted diseases under classical transmission-virulence trade-offs (Castillo-  
235 Chavez and Velasco-Hernández 1998). While we found lower mean virulence in scenarios  
236 with asynchronous host resources, the landscape heterogeneity was the main driver of  
237 virulence evolution. Interestingly, under asynchrony, we found higher proportions of low and  
238 high strains coexisting in homogeneous landscapes, indicating that isolated disease hotspots  
239 (Kürschner et al. 2021) could facilitate the persistence of different viral strains.

240 As long as host populations in our model are distributed heterogeneously, mean pathogenic  
241 virulence remains similar, with little change from completely heterogeneous, i.e., random  
242 landscapes, to the less heterogeneous medium habitat clusters. However, in large clusters, a  
243 clear increase in mean virulence was apparent, showing that there is a threshold in landscape  
244 homogeneity not only enhancing disease spread, but also evolution towards higher virulence.  
245 These modelling findings are consistent with previous research on thresholds in disease  
246 transmission and functional connectivity. For example, homogenous landscapes have been  
247 shown to facilitate the spread of rabies in raccoons (*Procyon lotor*) (Brunker et al. 2012) or  
248 tuberculosis in badgers (*Meles meles*) (Acevedo et al. 2019), while more heterogeneous  
249 landscapes have been shown to limit the spread of highly virulent pathogens (Lane-deGraaf  
250 et al. 2013 p.). Host-pathogen interactions — in directly transmitted diseases — occur at  
251 specific locations and points in time, with the spatial and temporal variability in the

252 availability of susceptible hosts being one of the governing factors of a successful  
253 transmission (Hudson 2002, Ostfeld et al. 2005, Real and Biek 2007). Consequently,  
254 homogenous landscapes and their lack of barriers allow more virulent pathogen strains to  
255 infect a sufficient number of hosts to persist in those landscapes. On the contrary, in  
256 heterogeneous landscapes, small clusters of high host density in a matrix of low density cause  
257 the extinction of highly virulent strains. This ‘dilution’ pattern can be explained by the short  
258 survival time of individuals in the matrix that form an immunity belt around the clusters and  
259 prevent spread between clusters (Marescot et al. 2021). Hence, in parallel with the ‘dilution  
260 hypotheses’ at the community scale, heterogeneous or ‘diverse’ landscapes provide less  
261 competent hosts for an epidemic (Patz et al. 2004, Civitello et al. 2015).

262 Increasing landscape homogenisation also resulted in higher mean virulence in scenarios with  
263 asynchrony between host life-history and resource availability (prediction 3). Even though  
264 overall susceptible host density was lower in asynchronous scenarios, the homogenous  
265 landscape’s increased connectivity allowed for higher virulent strains to persist at high  
266 prevalence. In the more homogenous, but still clustered, landscape, composed of large areas  
267 of high habitat suitability, the virulence of occurring strains was similar between the  
268 scenarios with and without synchrony. This indicates a strong effect of landscape  
269 configuration.

270 Interestingly, in our previous study (Kürschner et al. 2021) , we showed that increasing  
271 spatial homogeneity of the landscape affected pathogen persistence negatively without  
272 pathogen virulence evolution. One reason behind this difference lies in the temporal  
273 differentiation of the strains within the landscapes. During the beginning of an outbreak, the  
274 pathogen strains with low virulence are able to spread across the landscape into larger habitat  
275 clusters due to the long survival times they impose on their hosts. Once the susceptible host



276 density in one of the neighbouring areas is high enough, highly virulent strains that  
277 previously only occurred in low prevalence outcompete the low virulent strains and increase  
278 in prevalence. In other words, when host density increases, the high virulence strains  
279 capitalize on the high possibility for transmission and are likely to become dominant (Altizer  
280 et al. 2006, Hite and Cressler 2018). However, although highly virulent strains became more  
281 dominant, lower virulent strains continued to persist within the host population. In line with  
282 our findings, the coexistence of high and low virulent strains was also shown for rabbit  
283 haemorrhagic disease in the United Kingdom (Forrester et al. 2009) as well as influenza A in  
284 wild birds (Olsen et al. 2006).

285 Furthermore, our results show that, independent of landscape heterogeneity, a single, low  
286 virulent strain of a pathogen is able to evolve into a complex system of multiple coexisting  
287 strains with varying virulence (prediction 1). However, while multiple strains coexisted at  
288 any given time throughout all tested scenarios, we demonstrated that some strains likely  
289 become dominant (prediction 2). Similarly, a system of coexisting low and highly virulent  
290 strains were reported by empirical studies of the African swine fever virus in wild boar  
291 (Portugal et al. 2015), a pathogen causing severe diseases with huge economic impact (Artois  
292 et al. 2002). In this system the carriers of low virulent strains could remain infectious over  
293 long periods of time (de Carvalho Ferreira et al. 2012) increasing the chance of the pathogen  
294 transmission and its mutation into higher virulent strains, which could become dominant over  
295 time. In our study, the virulence of the dominant strain was intrinsically linked to the degree  
296 of landscape homogenisation but was also variable in time. Our findings are consistent with  
297 theoretical models that showed an increase of pathogenic virulence over time (Osnas et al.  
298 2015). However, while Osnas et al. (2015) assumed a direct trade-off between virulence and  
299 host movement in homogenous landscapes, here we show that different landscape

300 configurations may lead to the same patterns of increasing virulence without the necessity of  
301 such a trade-off.

302 On the one hand, our results show that with natural landscapes becoming more fragmented  
303 and resources becoming more asynchronous due to global change, a shift towards lower  
304 virulent pathogens could be expected. As a consequence, some diseases may become  
305 endemic in their respective host populations. The longer a pathogen is able to persist within  
306 its host population the higher the risk for spontaneous mutations and the possibility of  
307 spillovers to other species. On the other hand, global change will lead to increasing  
308 homogenisation within those fragments (Patz et al. 2004) and has the potential to increase the  
309 average pathogenic virulence with possibly catastrophic effects on wildlife communities. A  
310 large variance in virulence has been shown among infected host individuals, where the  
311 infection can range from severe to asymptomatic. This variation can be the result of a variety  
312 of factors, including genetic variation or intraspecific host interactions but also environmental  
313 conditions (Ebert and Bull 2003). Furthermore, an increase in virulence will go hand in hand  
314 with higher transmission rates in many diseases (Messinger and Ostling 2009, Alizon and  
315 Michalakis 2015) that will increase the probability of pathogen spillovers even more. While  
316 pathogen spillovers to other wild or domestic animal populations can have profound social or  
317 economic effects (Kamo et al. 2007), the possibly detrimental effects on human health cannot  
318 be underestimated. The current SARS-CoV-2 pandemic clearly highlights the importance of  
319 understanding which factors govern the spread of diseases in wildlife populations and how  
320 anthropogenic changes may alter those in the future.

321

## 322 Methods

### 323 Model overview

324 We modified a spatially explicit individual-based, eco-epidemiological model developed by  
325 Kürschner et al. (2021). It is based on earlier models considering neighbourhood infections  
326 only that was developed by Kramer-Schadt et al. (2009), Lange et al. (2012a, b) and Scherer  
327 et al. (2020) and includes spatiotemporal landscape dynamics representing changing resource  
328 availability, coupled with resource-based mortality. We incorporated evolution of viral traits  
329 such as virulence and corresponding trade-offs with viral transmission (see below). A  
330 complete and detailed model description following the ODD (Overview, Design concepts,  
331 Detail) protocol (Grimm et al. 2006, 2010) is provided in the supplementary material and the  
332 model (implementation) in the Zenodo Database and on GitHub [links provided on  
333 acceptance].

334

335 The model comprises three main components, a host model depending on underlying  
336 landscape features, an epidemiological pathogen model and a pathogen evolutionary model.  
337 Host individuals are characterised by sex, age, location, demographic status (residential,  
338 dispersing) and epidemiological status (susceptible, infected, immune). The epidemiological  
339 status of the individuals is defined by an SIR epidemiological classification (susceptible,  
340 infected, and recovered; Kermack and McKendrick 1927)). The pathogen is characterized by  
341 strain type, virulence and transmission. The pathogen model alters host survival rates and  
342 infection length depending on the pathogen's virulence, while the dynamic landscape features  
343 determine host reproductive success. We record strain occurrences as the number of infected  
344 individuals carrying a specific strain and pathogen persistence, measured at the level of  
345 simulation runs (see below).

346 Pathogen dynamics

347 We determined the course of the disease by an age-specific case fatality rate and a strain-  
348 specific infectious period. Highly virulent strains are characterized by a short infectious  
349 period and low virulent strains by a long infectious period. Transiently infected hosts shed the  
350 pathogen for one week and gain lifelong immunity (Dahle and Liess 1992). Infection  
351 dynamics emerge from multiple processes: within-group transmission and individual age-  
352 dependent courses of infection. Within groups, the density-dependent infection pressure (i.e.  
353 the chance of a host individual to become infected) is determined by a transmission chance  
354 and the number of infectious group members carrying the same strain. In this model we  
355 included the dependence of the transmission chance on the strain's virulence, so that the  
356 strains with higher virulence have higher transmission chance. Furthermore, we modified the  
357 density dependence of the infection pressure to be strain-specific to accommodate a lower  
358 per-strain infection density for the following reason: The original model based on a single  
359 pathogen strain used the density of infected individuals in a cell to infer the likelihood for a  
360 susceptible host in that cell to become infected based on a binomial model. Our model  
361 allows the evolution into 12 (arbitrarily categorized) different viral strains. The infection  
362 pressure  $\lambda$ , i.e. the probability of pathogen transmission to a susceptible host individual, is  
363 determined for each strain individually. Differences in strain transmissibility are added to the  
364 strain specific infection pressure through  $T_s$  (1). The probability  $\lambda_{is}$  of an individual  $i$  of being  
365 infected by a specific strain  $s$  is calculated as

366 
$$\lambda_{is} = I - (I - \beta_w + T_s)^{I_{js}} * (I - \frac{\beta_w + T_s}{10})^{\Sigma I_{js}} \quad (1)$$

367 with  $\beta_w$  being the individual probability of transmission to the power of all infected  
368 individuals  $I_{js}$  in a group  $j$  per strain  $s$  as well as a reduced transmission probability between  
369 groups (i.e. cells)  $\frac{\beta_w}{10}$  to the power of all infected individuals in neighboring groups  $\Sigma I_{js}$ .

370 The strain virulence translates directly into infection length, i.e., host survival time, where a  
371 high virulence results in shorter survival times for the host compared to low-virulence.  
372 Consequently, the shorter lifetime of a highly virulent pathogen results in a shorter  
373 reproductive time span, while making the pathogen highly infective.

374 *Evolution of pathogenic traits* – Virulence and transmission are emergent properties and are  
375 evolving in the model. This means, while the position of each of the 12 strains on the  
376 transmission trade-off-curve is fixed, the selection of each strain during a transmission event  
377 is variable. Our trade-off curve is modelled to follow theoretical transmission-virulence  
378 trade-off curves (Alizon et al. 2009) and is applied for each infected host individually.  
379 During a transmission event, a strain can, with a mutation rate of 0.01, mutate into a new  
380 strain with a different virulence. The virulence of the new strain is selected from a normal  
381 distribution with a standard deviation  $\sigma = 1$  around the virulence value of the originally  
382 transmitted strain, meaning that the new strain will be closely related to the parental strain.

### 383 Landscape structure and dynamics

384 The tested landscapes consist of a spatial grid of 1.250 2 km x 2 km cells, each representing  
385 the average home range of a social host, e.g. a wild boar group (Kramer-Schadt et al. 2009) ,  
386 totalling a 100 km x 50 km landscape. The landscapes are self-contained systems without any  
387 outside interaction. Each cell is characterized by a variable resource availability that  
388 represents host breeding capacity and translates directly into host group size, with the  
389 minimum being one breeding female per group to a maximum of nine. Resource availability  
390 was adapted to achieve the average wild boar density of five breeding females per km<sup>2</sup>  
391 (Howells and Edwards-Jones 1997, Sodeikat and Pohlmeier 2003, Melis et al. 2006). We  
392 investigated several landscape scenarios of varying spatial complexity, ranging from a fully

393 random landscape structure to different degrees of random landscape clusters generated in R  
394 (R Core Team 2020) using the NLMR package (Sciaini et al. 2018) up to a fully  
395 homogeneous landscape. To exclude any biases that could stem from different host densities,  
396 the mean female breeding capacity was kept constant at five females per km<sup>2</sup> across the  
397 different landscape types (Supplementary material Appendix Fig. B1). The spatiotemporal  
398 landscape dynamics that were designed to mimic seasonal changes in resource availability by  
399 gradually increasing and decreasing resource availability were kept unchanged from the  
400 previous model implementation by Kürschner et al. (2021).

#### 401 Process overview and scheduling

402 The temporal resolution of the model equals the approximate pathogen incubation time of  
403 one week (Artois et al. 2002). The model procedures were scheduled each step in the  
404 following order: pathogen transmission, pathogen evolution, natal host group split of subadult  
405 males and females, resource-based host dispersal, host reproduction, baseline host mortality,  
406 strain-based host mortality, resource-based host mortality, host ageing and landscape  
407 dynamics. Natal group split of males and females was limited to week 17 and week 29 of  
408 each year, respectively, representing the observed dispersal time for each sex.

409 *Host mortality* – Mortality in response to resource availability remained unchanged to the  
410 previous model implementation (for details see ODD in the supplementary material).

411 Additionally, we added a fixed, strain-specific mortality for each strain that affects the host  
412 population.

413 *Landscape dynamics with temporal lag* – We modelled two levels of temporal lag ( $t_{lag}$ )  
414 implemented in Kürschner et al. (2021). We focus on the level 0% (synchrony between host  
415 population dynamics and resource availability) to 100% (asynchrony between host population

416 dynamics and resource availability), with the latter simulating phenological mismatch  
417 between the resources and hosts reproduction potentially due to climate change. The extreme  
418 values were chosen because previous studies investigating temporal lag did not show strong  
419 effects in the intermediary steps (Kürschner et al. 2021).

#### 420 Model analysis

421 Each simulation was run for 100 years in total, with the virus released in a randomly taken  
422 week of the second year (week 53–104), to allow the population to stabilize after  
423 initialization. The virus was introduced to a set of multiple predefined cells in the centre of  
424 the landscape to ensure an outbreak. The virus was released in a low virulence variant. We  
425 ran 25 repetitions per combination of landscape scenarios (5 levels: small clusters, medium  
426 clusters, large clusters, homogenous landscape and random) and asynchrony (2 levels:  $t_{lag}$  0%,  
427  $t_{lag}$  100%). We also analysed the strain occurrence (i.e., if a strain was present in any  
428 landscape cell, recorded at every timestep) and number of infected hosts per strain at every  
429 timestep to measure strain extinction as well as reappearance through mutation. We further  
430 recorded the proportion that each strain contributed to the pool of infected hosts by  
431 calculating the ratio of the hosts infected with each strain to the total number of hosts infected  
432 with all strains, at each time step. To highlight differences in strain composition in those  
433 scenarios, we subtracted the mean strain proportion in asynchronous scenarios from the mean  
434 proportion in synchronous scenarios. We categorized all viral strains into three categories:  
435 low virulence strains; medium virulence strains; high virulence strains, each compartment  
436 summing the outcomes of 4 of the 12 strains modelled.

437

438 Acknowledgements

439 This work was supported by the German Research Foundation (DFG) in the framework of the  
440 BioMove Research Training Group (DFG-GRK 2118/1). We thank Volker Grimm for  
441 valuable comments on earlier drafts of this manuscript and Florian Jeltsch and Heribert Hofer  
442 for helpful discussions.

443 Statement of authorship

444 All authors agree to submission of the manuscript, and each author carries a degree of  
445 responsibility for the accuracy, integrity and ethics of the manuscript and works described  
446 therein.

447 Author contributions

448 TK and SKS developed the core idea and designed the study. TK rewrote and modified the  
449 simulation model together with CS and SKS. TK, VR, and SKS analysed the simulation  
450 results. TK is the lead author and CS, VR, NB and SKS contributed substantially to the  
451 writing. All authors agreed to submission of the manuscript, and each author is accountable  
452 for the aspects of the conducted work and ensures that questions related to the accuracy or  
453 integrity of any part of the work are appropriately investigated and resolved.

454

455 References

- 456 Acevedo, P. et al. 2019. Tuberculosis Epidemiology and Badger (*Meles meles*) Spatial  
457 Ecology in a Hot-Spot Area in Atlantic Spain. - *Pathogens* 8: 292.
- 458 Alizon, S. and Michalakis, Y. 2015. Adaptive virulence evolution: the good old fitness-based  
459 approach. - *Trends in Ecology & Evolution* 30: 248–254.
- 460 Alizon, S. et al. 2009. Virulence evolution and the trade-off hypothesis: history, current state  
461 of affairs and the future. - *Journal of evolutionary biology* 22: 245–259.



- 462 Altizer, S. et al. 2006. Seasonality and the dynamics of infectious diseases. - Ecology letters  
463 9: 467–484.
- 464 Anderson, R. M. and May, R. M. 1982. Coevolution of hosts and parasites. - Parasitology 85:  
465 411–426.
- 466 Artois, M. et al. 2002. Classical swine fever (hog cholera) in wild boar in Europe. - Rev. Sci.  
467 Tech. OIE 21: 287–303.
- 468 Boots, M. 2004. Large Shifts in Pathogen Virulence Relate to Host Population Structure. -  
469 Science 303: 842–844.
- 470 Boots, M. and Meador, M. 2007. Local Interactions Select for Lower Pathogen Infectivity. -  
471 Science 315: 1284–1286.
- 472 Brunker, K. et al. 2012. Integrating the landscape epidemiology and genetics of RNA  
473 viruses: rabies in domestic dogs as a model. - Parasitology 139: 1899–1913.
- 474 Castillo-Chavez, C. and Velasco-Hernández, J. X. 1998. On the Relationship Between  
475 Evolution of Virulence and Host Demography. - Journal of Theoretical Biology 192:  
476 437–444.
- 477 Choua, M. and Bonachela, J. A. 2019. Ecological and Evolutionary Consequences of Viral  
478 Plasticity. - The American Naturalist 193: 346–358.
- 479 Civitello, D. J. et al. 2015. Biodiversity inhibits parasites: Broad evidence for the dilution  
480 effect. - Proc. Natl. Acad. Sci. U.S.A. 112: 8667–8671.
- 481 Cressler, C. E. et al. 2016. The adaptive evolution of virulence: a review of theoretical  
482 predictions and empirical tests. - Parasitology 143: 915–930.
- 483 Dahle, J. and Liess, B. 1992. A review on classical swine fever infections in pigs:  
484 Epizootiology, clinical disease and pathology. - Comparative Immunology,  
485 Microbiology and Infectious Diseases 15: 203–211.
- 486 Day, T. 2003. Virulence evolution and the timing of disease life-history events. - Trends in  
487 Ecology & Evolution 18: 113–118.
- 488 Day, T. and Gandon, S. 2007. Applying population-genetic models in theoretical evolutionary  
489 epidemiology. - Ecol Letters 10: 876–888.
- 490 de Carvalho Ferreira, H. C. et al. 2012. African swine fever virus excretion patterns in  
491 persistently infected animals: A quantitative approach. - Veterinary Microbiology 160:  
492 327–340.
- 493 Adaptive dynamics of infectious diseases: in pursuit of virulence management 2005. (U  
494 Dieckmann, JAJ Metz, M Sabelis W, and K Sigmund, Eds.). - Cambridge University  
495 Press.
- 496 Ebert, D. and Bull, J. J. 2003. Challenging the trade-off model for the evolution of virulence:  
497 is virulence management feasible? - Trends in Microbiology 11: 15–20.

- 498 Forrester, N. L. et al. 2009. Co-circulation of widely disparate strains of Rabbit haemorrhagic  
499 disease virus could explain localised epidemicity in the United Kingdom. - *Virology*  
500 393: 42–48.
- 501 Galvani, A. P. 2003. Epidemiology meets evolutionary ecology. - *Trends in Ecology &*  
502 *Evolution* 18: 132–139.
- 503 Geoghegan, J. L. and Holmes, E. C. 2018. The phylogenomics of evolving virus virulence. -  
504 *Nat Rev Genet* 19: 756–769.
- 505 Griette, Q. et al. 2015. Virulence evolution at the front line of spreading epidemics. -  
506 *Evolution* 69: 2810–2819.
- 507 Grimm, V. et al. 2006. A standard protocol for describing individual-based and agent-based  
508 models. - *Ecological Modelling* 198: 115–126.
- 509 Grimm, V. et al. 2010. The ODD protocol: A review and first update. - *Ecological Modelling*  
510 221: 2760–2768.
- 511 Hite, J. L. and Cressler, C. E. 2018. Resource-driven changes to host population stability  
512 alter the evolution of virulence and transmission. - *Phil. Trans. R. Soc. B* 373:  
513 20170087.
- 514 Howells, O. and Edwards-Jones, G. 1997. A feasibility study of reintroducing wild boar *Sus*  
515 *scrofa* to Scotland: Are existing woodlands large enough to support minimum viable  
516 populations. - *Biological Conservation* 81: 77–89.
- 517 *The ecology of wildlife diseases 2002.* (PJ Hudson, Ed.). - Oxford University Press.
- 518 Kamo, M. et al. 2007. The role of trade-off shapes in the evolution of parasites in spatial host  
519 populations: An approximate analytical approach. - *Journal of Theoretical Biology*  
520 244: 588–596.
- 521 Kermack, W. O. and McKendrick, A. G. 1927. A Contribution to the Mathematical Theory of  
522 Epidemics. - *Proceedings of the Royal Society A: Mathematical, Physical and*  
523 *Engineering Sciences* 115: 700–721.
- 524 Kramer-Schadt, S. et al. 2009. Individual variations in infectiousness explain long-term  
525 disease persistence in wildlife populations. - *Oikos* 118: 199–208.
- 526 Kürschner, T. et al. 2021. Movement can mediate temporal mismatches between resource  
527 availability and biological events in host–pathogen interactions. - *Ecol. Evol.* 11:  
528 5728–5741.
- 529 Lane-deGraaf, K. E. et al. 2013. A test of agent-based models as a tool for predicting  
530 patterns of pathogen transmission in complex landscapes. - *BMC Ecol* 13: 35.
- 531 Lange, M. et al. 2012a. Disease severity declines over time after a wild boar population has  
532 been affected by classical swine fever—legend or actual epidemiological process? -  
533 *Preventive veterinary medicine* 106: 185–195.
- 534 Lange, M. et al. 2012b. Efficiency of spatio-temporal vaccination regimes in wildlife  
535 populations under different viral constraints. - *Veterinary Research* 43: 37.

- 536 Lebarbenchon, C. et al. 2008. Evolution of pathogens in a man-made world. - *Molecular*  
537 *Ecology* 17: 475–484.
- 538 Lenski, R. E. and May, R. M. 1994. The Evolution of Virulence in Parasites and Pathogens:  
539 Reconciliation Between Two Competing Hypotheses. - *Journal of Theoretical Biology*  
540 169: 253–265.
- 541 Marescot, L. et al. 2021. 'Keeping the kids at home' can limit the persistence of contagious  
542 pathogens in social animals. - *J Anim Ecol* 90: 2523–2535.
- 543 Melis, C. et al. 2006. Biogeographical variation in the population density of wild boar (*Sus*  
544 *scrofa*) in western Eurasia. - *J Biogeography* 33: 803–811.
- 545 Messinger, S. M. and Ostling, A. 2009. The consequences of spatial structure for the  
546 evolution of pathogen transmission rate and virulence. - *The American naturalist* 174:  
547 441–454.
- 548 Olsen, B. et al. 2006. Global Patterns of Influenza A Virus in Wild Birds. - *Science* 312: 384–  
549 388.
- 550 Osnas, E. E. et al. 2015. Evolution of Pathogen Virulence across Space during an Epidemic.  
551 - *The American Naturalist* 185: 332–342.
- 552 Ostfeld, R. et al. 2005. Spatial epidemiology: an emerging (or re-emerging) discipline. -  
553 *Trends in Ecology & Evolution* 20: 328–336.
- 554 Patz, J. A. et al. 2004. Unhealthy Landscapes: Policy Recommendations on Land Use  
555 Change and Infectious Disease Emergence. - *Environmental Health Perspectives*  
556 112: 1092–1098.
- 557 Portugal, R. et al. 2015. Related strains of African swine fever virus with different virulence:  
558 genome comparison and analysis. - *Journal of General Virology* 96: 408–419.
- 559 R Core Team 2020. R: A Language and Environment for Statistical Computing. - R  
560 Foundation for Statistical Computing.
- 561 Real, L. A. and Biek, R. 2007. Spatial dynamics and genetics of infectious diseases on  
562 heterogeneous landscapes. - *J. R. Soc. Interface.* 4: 935–948.
- 563 Scherer, C. et al. 2020. Moving infections: individual movement decisions drive disease  
564 persistence in spatially structured landscapes. - *Oikos*: oik.07002.
- 565 Sciaini, M. et al. 2018. NLMR and landscapetools : An integrated environment for simulating  
566 and modifying neutral landscape models in R (N Golding, Ed.). - *Methods Ecol Evol*  
567 9: 2240–2248.
- 568 Sodeikat, G. and Pohlmeier, K. 2003. Escape movements of family groups of wild boar *Sus*  
569 *scrofa* influenced by drive hunts in Lower Saxony, Germany. - *Wildlife Biology* 9: 43–  
570 49.
- 571 Tasakis, R. N. et al. 2021. SARS-CoV-2 variant evolution in the United States: High  
572 accumulation of viral mutations over time likely through serial Founder Events and  
573 mutational bursts (YE Khudyakov, Ed.). - *PLoS ONE* 16: e0255169.

574 Visher, E. et al. 2021. The three Ts of virulence evolution during zoonotic emergence. - Proc.  
575 R. Soc. B. 288: 20210900.

576 Wilcox, B. A. and Gubler, D. J. 2005. Disease ecology and the global emergence of zoonotic  
577 pathogens. - Environ Health Prev Med 10: 263.

578